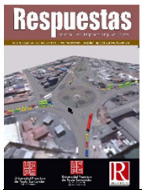

Respuestas
Journal of Engineering Sciences
RESPUESTAS

Original Article https://doi.org/10.22463/0122820X.2824

Study of the influence of material properties in the energy conversion process of thermoelectric generators for waste heat recovery applications

Estudio de la influencia de las propiedades del material en el proceso de conversión de energía de generadores termoeléctricos para aplicaciones de recuperación de calor

Byron Medina-Delgado[1], Guillermo Valencia-Ochoa[2], Jorge Duarte-Forero[3]

[1*]*Doctor en Ciencias, byronmedina@ufps.edu.co, ORCID: 0000-0003-0754-8629, Universidad Francisco de Paula Santander, Cúcuta, Colombia.*
[2]*Doctor en Ingeniería, guillermoevalencia@mail.uniatlantico.edu.co, ORCID: 0000-0001-5437-1964, Universidad del Atlántico, Barranquilla, Colombia.*
[3]*Doctor en Ingeniería Mecánica, jorgeduarte@mail.uniatlantico.edu.co, ORCID: 0000-0001-7345-9590, Universidad del Atlántico, Barranquilla, Colombia.*

How to cite: B. Medina-Delgado, G. Valencia-Ochoa and J. Duarte-Forero, "Study of the influence of material properties in the energy conversion process of thermoelectric generators for waste heat recovery applications". *Respuestas,* vol. 25, no. 3, pp. 95-108, 2020.

Received on June 22, 2020 - Approved on October 23, 2020.

ABSTRACT

The present study analyzed the effect of material properties in the energy conversion process of Thermoelectric Generators (TEGs). For the development of the study, two materials whose properties vary with respect to temperature (Bi0.4Sb1.6Te3 and Cu11NiSb4S13) and a material with constant properties (Bi2Te3) were analyzed. Through numerical simulation processes, each material was subjected to different temperature differences to monitor the effect on the electrical output power, heat flux, and energy conversion efficiency. The results showed that neglecting the temperature dependence produces higher or lower performance estimations depending on the temperature levels experienced by the TEG. Overall, the material Bi2Te3 displayed 35% more electrical power output and conversion efficiency compared to the Bi0.4Sb1.6Te3 material. Therefore, considering the variability of thermoelectric materials demonstrated to be essential to obtain realistic process performance. Also, the heat flux produced by the Fourier effect presents the most significant impact on the electrical power generation of the TEG. Among materials with variable properties, the Bi0.4Sb1.6Te3 increases the conversion efficiency up to 25% compared to the Cu11NiSb4S13. In conclusion, the study of material properties using numerical simulations emerged as a robust and practical tool to evaluate TEG performance.

Keywords:

Efficiency,
Energy conversion,
Material properties,
Output power,
Thermoelectric generators.

RESUMEN

En el presente estudio, se propone un análisis del efecto de las propiedades del material en el proceso de conversión de energía de generadores termoeléctricos (GTE). En el desarrollo del estudio, se analizaron dos materiales cuyas propiedades varían con respecto a la temperatura (Bi0.4Sb1.6Te3 y Cu11NiSb4S13) y un material de propiedades constantes (Bi2Te3). A través del proceso de simulación, cada material se sometió a variaciones de temperatura para monitorear su efecto en variables tales como la generación eléctrica, flujo de calor y eficiencia de conversión energética. Los resultados obtenidos mostraron que, al considerar la dependencia de la temperatura del material se obtienen estimaciones mayores o menores dependiendo en el nivel de temperatura experimentado por el GTE. De manera general, el material Bi2Te3 incrementó la generación de electricidad y la eficiencia hasta en un 35 % comparado al material Bi0.4Sb1.6Te3. De tal forma, se demostró que considerando la variabilidad del material del GTE es esencial para obtener resultados realistas del proceso de conversión energético. Por otro lado, el flujo de calor producido por el efecto de Fourier mostró el mayor impacto en la generación de electricidad del GTE. Dentro de los materiales con propiedades variables, el material Bi0.4Sb1.6Te3 incrementó la eficiencia de conversión hasta en un 25% en comparación con el Cu11NiSb4S13. Finalmente, el estudio de las propiedades de los materiales para la construcción de GTEs usando simulaciones numéricas demostró ser una herramienta robusta y práctica para evaluar el desempeño de este dispositivo.

Palabras clave:

Conversión energética,
Eficiencia,
Generadores termoeléctricos,
Potencia de salida,
Propiedades de material.

***Corresponding author.**
E-mail Address: *byronmedina@ufps.edu.co* (Byron Medina-Delgado)

Introduction

Although the world is becoming increasingly aware of the importance of protecting the environment, the use of fossil fuels remains the main source of energy supply [1], [2]. As a consequence, greenhouse emissions produced by energy systems powered by fossil fuels represent a socio-environmental problem. Therefore, the main focus of both industry and academics centers on reducing fossil fuel consumption and global emissions through the continuous optimization of the overall performance of the processes that involve their use [3]-[6].

Statistical studies show that only 30-35% of the energy produced in power plants is used in a useful way; the rest is lost in the form of residual heat [7]. Hence, Waste Heat Recovery (WHR) technologies stand as a promising strategy to implement in different energy systems [4], [5]. Mukherjee et al. [8] studied the capacity of a heat recovery system through the interaction of gases in an industrial process of food manufacturing. Ganguly et al. [9] investigated alternatives to improve the efficiency of a solar panel system by recovering heat. Particularly, Thermoelectric Generators (TEG) has gained notoriety for integration in energy recovery processes due to various advantages such as zero-polluting emissions, low weight, absence of moving parts, minimal noise, and little maintenance requirement [10]-[13]. The use of these devices has been extended in different applications. Wang et al. [14] designed a TEG to directly transform heat released from the human body into electricity, which could be used to monitor body movement. Allouhi et al. [15] theoretically studied heating systems that integrate TEGs. The results obtained showed that the TEG heating system allows an average energy saving of 60% compared to conventional heaters. Lertsatitthanakorn [16] investigated the use of TEG devices in processes involving biomass as fuel. The results reported that a temperature difference of 150 °C generates 2.4 W of electrical power. Overall, previous studies demonstrated the potential of TEGs for WHR applications. However, the exploration of material properties in the TEG performance is rarely characterized, despite being a promising avenue to improve the efficiency of the energy conversion process. The materials commonly used for TEGs construction include bismuth telluride and lead telluride [17], [18]. In recent years, researchers have focused their attention on synthetic materials through processes such as mechanical alloys [19], fusion [20], microwave synthesis [21], and hydrothermal [22]. The materials mentioned above are incorporated since they feature lower thermal conductivity and a higher merit (ZT) coefficient [23].

Numerical simulations facilitate research on thermoelectric generators and especially on the characterization of material properties influence as it can be implemented as an initial stage to evaluate the overall performance of different design proposals. This methodology fosters cost savings since testing tasks are significantly reduced. Fernández et al. [24] studied the influence of the size and internal shape of TEGs on their energy recovery capacity by using computational fluid dynamics (CFD). Muralidhar et al. [25] investigated different alternatives to optimize heat transfer between TEGs and the exhaust gases of a vehicular engine using CFD tools. Table I listed different investigations focused on studying thermoelectric materials using numerical simulations and the main outcomes.

Table I. Study of thermoelectric materials using numerical simulations

Material	Observations
Bismuth telluride	The proposed thermal resistance model presented an overestimation of the performance of the TEG [26].
Sb_2Te_3 and Bi_2Te_3	The material manages to maintain adequate performance when fluctuations in temperature occur on the surfaces of the TEG [27].
TEG 1-199-1.5-1.8-250.	Increasing the thickness of the metal foam causes an increase in the output power of the TEG [28].
Bi_2Te_3	Using TEG is a viable way to recover some of the thermal energy from the engine exhaust gases [24].

Despite the advantages provided by the use of numerical methods, many of the studies that involve the analysis of thermoelectric materials assume the properties of the material to be constant, which simplifies the calculation and the physical problem [29]. However, the thermoelectric properties of the materials for TEG construction are temperature

dependent. Among these properties are the Seebeck coefficient, thermal conductivity, and electrical resistivity. Some research indicates that ignoring this temperature dependence leads to erroneous estimations on the performance capacity of TEGs [30]. Wang et al. [31] observed that assuming a model with constant properties causes a lower estimate of the potential for energy recovery. Meng et al. [32] demonstrated that models with variable properties allow better precision at high operating temperatures.

Previous research agreed that assuming constant material properties can lead to serious errors in estimating TEG conversion efficiency. Therefore, the present study proposes an analysis of the electrical power generation and efficiency performance of TEGs when operating with different thermoelectric materials, whose properties are temperature-dependent. In this sense, this work contributes to close the knowledge gap regarding TEG performance characterization from the material properties criteria. Accordingly, two different materials with variable properties are evaluated using CFD numerical simulations and further compared with constant property material.

Materials and methods

Geometric model TEG

For the present study, the geometric model of the TEG is composed of 130 thermoelectric pairs. This number of thermoelectric pairs was chosen based on similar TEG applications. Each pair is made up of two types of semiconductor materials (P-type and N-type). The dimensions of these semiconductors are 2mm x 2mm x 2mm in high, wide, and long, respectively. The overall dimensions of the TEG are 40mm x 40mm in width and length. Figure 1 illustrates the configuration of the thermoelectric pairs.

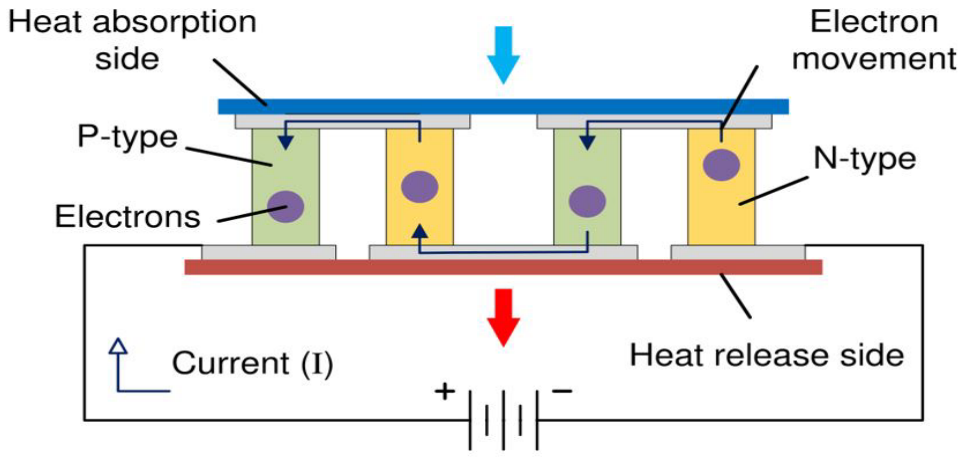

Figure 1. Thermoelectric pairs

Mathematical model

TEGs experience two types of physical phenomena in their operation, which correspond to electrical and thermal effects. The constitutive formulation that describes the operation of a TEG is described below. First, heat flow expression is defined as:

$$\dot{q} = \nabla \cdot \vec{q} \qquad (1)$$

where $\dot{q}$ and q are the heat generation and the heat flux vector, respectively. The TEG electric charge is set as:

$$0 = \nabla \cdot \vec{J} \quad (2)$$

where J is the electric current density. Thermal and electrical effects can be associated with each other [31], as indicated by Equation (3-4).

$$\vec{J} = -\frac{1}{\rho} \cdot (\nabla\varphi + S \cdot \nabla T) \quad (3)$$

$$\vec{q} = ST \cdot \vec{J} - k \cdot \nabla T \quad (4)$$

where $S,k,T,\rho,$ and φ are the Seebeck coefficient, thermal conductivity, temperature, electrical resistivity, and scalar electric potential, respectively. By unifying Equation (1-4), the equations that govern the behavior of thermoelectric generators can be expressed as:

$$0 = \nabla \cdot \left(\frac{1}{\rho} \cdot \nabla\varphi\right) + \nabla \cdot \left(\frac{S}{\rho} \cdot \nabla T\right) \quad (5)$$

$$\dot{q} = \nabla \cdot \left(ST\vec{J}\right) - \nabla \cdot (k \cdot \nabla T) \quad (6)$$

When a temperature difference occurs between the hot surface and the cold surface of the TEG, an electric current is generated, which can be defined as:

$$I = \frac{S \cdot \nabla T}{R_{load} + R_{TE}} \quad (7)$$

where R_{load} and R_{TE} are the external load resistance and the electrical resistance of the thermoelectric pair, respectively. The electrical output power can be set, as shown in Equation (8).

$$P_{elec} = \frac{R_{load}(S \cdot \nabla T)^2}{(R_{load} + R_{TE})^2} \quad (8)$$

When the resistance of the external load (R_{load}) equals the internal electrical resistance of the TEG (R_{TE}), the maximum electrical power generated is produced. This coincidence in the resistances is stable for the simulation process.

Numerical model

The open-source software OpenFOAM was used to study thermoelectric phenomena in the TEG. It is assumed that the thermoelectric pair is electrically connected in series and thermally in parallel with the rest of the elements of

the TEG. This allows the calculation of the power, heat flow, and total efficiency of the TEG, based on the study of a single thermoelectric pair and its multiplication by the total number of pairs.

Three different materials commonly used in the construction of thermoelectric modules were simulated in the study. The properties of these materials are shown in Table II, whereas Figure 2 shows the geometric model of the thermoelectric pair used as the basis for the simulations.

Table II. Test materials

Material	Property
$Cu_{11}NiSb_4S_{13}$ [33]	$k_p = k_n = 0.272 \times 10^{-9} \cdot T^3 - 1.660 \times 10^{-6} \cdot T^2 + 2.113 \times 10^{-3} \cdot T - 0.091$
	$\rho_p = \rho_n = 2.378 \times 10^{-8} \cdot T^3 + 1.061 \times 10^{-4} \cdot T^2 - 0.102 \cdot T + 358.413$
	$S_p = -S_n = 2.762 \times 10^{-13} \cdot T^3 - 6.603 \times 10^{-10} \cdot T^2 + 5.864 \times 10^{-7} \cdot T + 4.095 \times 10^{-5}$
$Bi_{0.4}Sb_{1.6}Te_3$ [34]	$k_p = k_n = 2.538 \times 10^{-9} \cdot T^3 + 9.568 \times 10^{-6} \cdot T^2 - 1.638 \times 10^{-3} \cdot T + 0.773$
	$\rho_p = \rho_n = -2.378 \times 10^{-8} \cdot T^3 + 1.061 \times 10^{-4} \cdot T^2 - 0.102 \cdot T + 358.413$
	$S_p = -S_n = 2.49 \times 10^{-13} \cdot T^3 - 3.560 \times 10^{-9} \cdot T^2 + 2.523 \cdot T - 2.200 \times 10^{-4}$
Bi_2Te_3 [35]	$k_p = k_n = 1.52$
	$\rho_p = \rho_n = 1.45 \times 10^{-5}$
	$S_p = -S_n = 0.227 \times 10^{-9}$

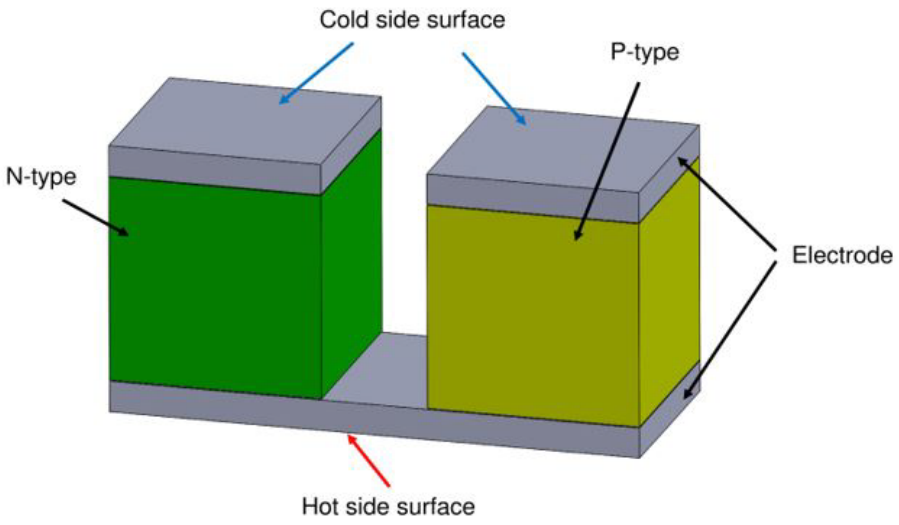

Figure 2. Thermoelectric pairs geometry

The description of the numerical simulation process used in this study is shown in Figure 3.

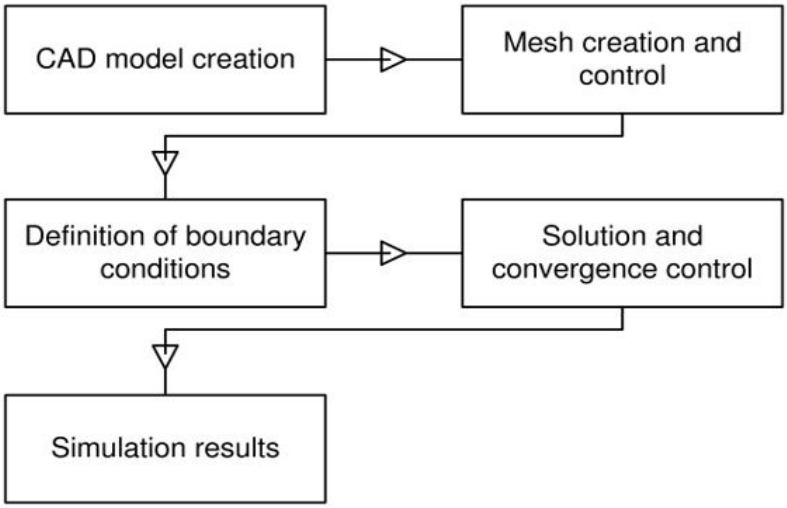

Figure 3. Simulation process scheme

For the numerical simulation process, a hexahedral mesh was selected since it was adequately adapted to the quadratic geometry of the thermoelectric pair. In order to determine the appropriate number of elements in the mesh, three types of mesh were simulated, which correspond to a coarse (4051 elements), medium (8754 elements), and fine (16743 elements) mesh. The results obtained in each type of mesh are compared with different levels of electrical power obtained experimentally. The results of this comparison are shown in Table III.

The results obtained in Table III show a closeness between the experimental and simulated data. However, it was observed that the use of fine mesh (16743 elements) presents a relative error of $\leq$1.5% compared to the experimental results. Therefore, the fine mesh is considered for the rest of the simulations.

Additionally, it is worth mentioning that the little difference between simulation and experimental results demonstrates the capacity of the numerical approach to obtain results in accordance with the actual conditions of the TEG.

Table III. Comparison between experimental and simulated data under different electrical power conditions

Experimental	Mesh type		
	Coarse	Medium	Fine
2 W	2.21	2.10	2.02
2.5 W	2.73	2.64	2.52
3 W	3.28	3.21	3.05
4 W	4.36	4.20	4.01

Results and Discussion

Effect of temperature difference on electrical power

The behavior of the electrical power of the TEG for the three materials as a function of the temperature difference is shown in Figure 4.

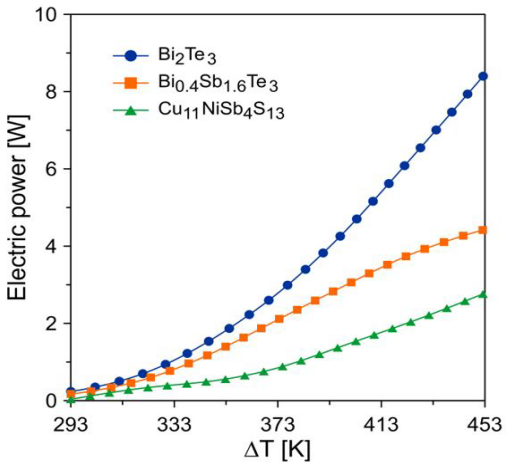

Figure 4. Distribution of electrical power as a function of temperature difference

The results show that the materials Bi2Te3, Bi0.4Sb1.6Te3, and Cu11NiSb4S13 tend to increase the electrical power generated as the temperature difference between the cold surface and the hot surface of the TEG increases. However, the Bi0.4Sb1.6Te3 material experiences a reduction in the power generated for temperature differences greater than 433 K, which indicates a decrease in TEG performance for high operating temperatures. However, the Bi0.4Sb1.6Te3 material generated approximately twice the power when compared to Cu11NiSb4S13.

Additionally, it was observed that the assumption of considering constant material properties produces an overestimation in the electrical power of the TEG. In the particular case of Bi2Te3, maximum electrical power was recorded twice and four times higher than that obtained in materials Bi0.4Sb1.6Te3 and Cu11NiSb4S13, respectively.

Effect of temperature difference on heat flux rate

The objective of thermoelectric modules is the transformation of thermal energy in the form of heat into electricity by using the Seebeck effect [36]. The heat flux experienced by thermoelectric pairs can be expressed as follows:

$$q = \frac{S \cdot I \cdot T_h}{A} - \frac{0.5I^2 \cdot R_{TE}}{A} + \frac{k \cdot \Delta T}{L_{TE}} \qquad (9)$$

where terms $\frac{S \cdot I \cdot T_h}{A}$, $\frac{0.5I^2 \cdot R_{TE}}{A}$ and $\frac{k \cdot \Delta T}{L_{TE}}$ indicate three heat flux types corresponding to the Peltier effect, Joule and Fourier, respectively [37]. To study the influence of these heat fluxes, their behavior is recorded as a temperature difference function. The results obtained are shown in Figure 5.

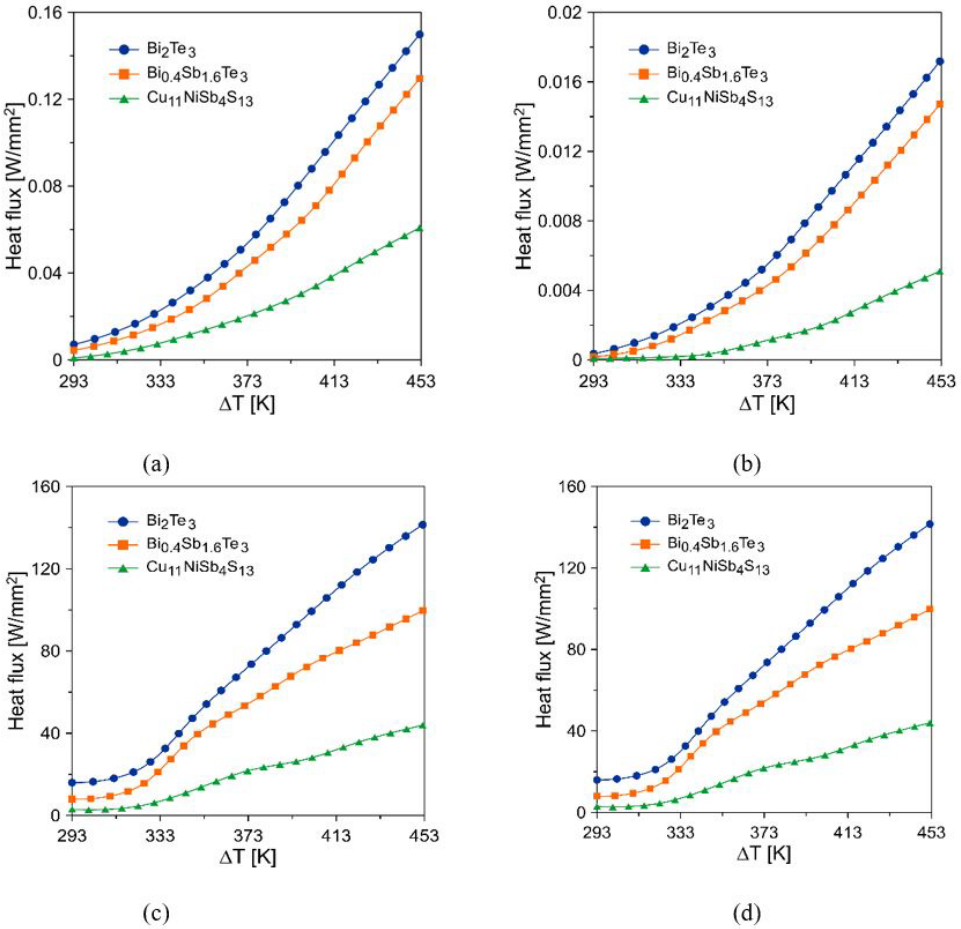

Figure 5. Distribution of heat fluxes from (a) Peltier, (b) Joule, (c) Fourier, and (d) total heat flux

Figure 5 shows that the Peltier and Joule effects increase exponentially with the temperature difference. In the case of the Fourier effect, linear growth was observed over a wide temperature range. For the analyzed range, a maximum heat flux range of 0.16 W/mm2, 0.018 W/mm2, and 140 W/mm2 were found for the Peltier, Joule, and Fourier effects, respectively. This shows a clear predominance of the Fourier effect over the other heat fluxes.

Electrical power curves

Figure 6 shows the distributions of the electrical power curves for the three materials at diverse temperature differences.

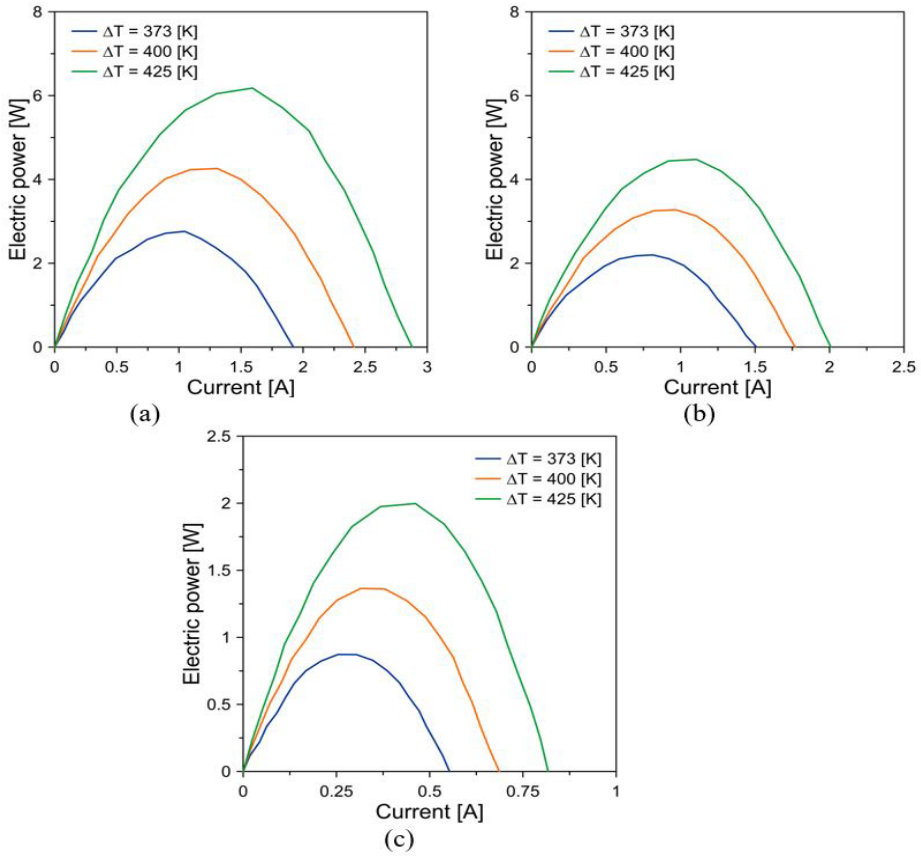

Figure 6. Electrical output power for material, (a) Bi_2Te_3, (b) $Bi0._4Sb_{1.6}Te_3$ and (c) $Cu_{11}NiSb_4S_{13}$

According to the results, an average increase of 25 K in the temperature difference causes an increase of 32%, 36%, and 39% in the power curve for the materials Bi2Te3, Bi0.4Sb1.6Te3, and Cu11NiSb4S13, respectively. When considering variable material properties, a reduction in the operating current range of the TEG is observed.

The analysis of the maximum points of the electrical power showed that the best operating range for materials Bi0.4Sb1.6Te3 and Cu11NiSb4S13 corresponds to a current interval between 0.5-1A and 0.25-0.375 A, respectively.

Energy conversion efficiency

The relationship between the conversion efficiency of the three materials with respect to the temperature difference is shown in Figure 7.

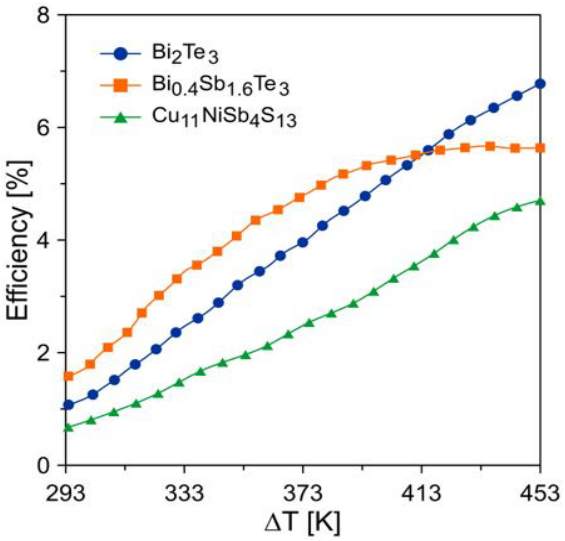

Figure.7. Energy conversion efficiency for different materials

The results obtained show that an increase in the temperature difference increases the energy conversion efficiency. For the material with constant properties, maximum efficiency of 7% is obtained. However, materials Bi0.4Sb1.6Te3 and Cu11NiSb4S13 reach a maximum efficiency level of 5% and 4%, respectively.

Unlike the linear increase in efficiency in materials Bi2Te3 and Cu11NiSb4S13, material Bi0.4Sb1.6Te3 shows a reduction in efficiency increase for temperature differences greater than 413 K. The above indicates that the ZT of the material is reduced.

Conclusions

In the present study, a numerical analysis using CFD tools was carried out to evaluate the influence of design materials on the overall performance of TEGs. The study proposed different scenarios for the analysis, namely: constant property material (Bi2Te3) and variable properties material (Bi0.4Sb1.6Te3 and Cu11NiSb4S13) with respect to the temperature.

In general, the material Bi2Te3 showed considerably higher performance compared to Bi0.4Sb1.6Te3 and Cu11NiSb4S13. This behavior is reflected in greater ranges of electrical power, current, and energy conversion efficiency. However, for temperature differences greater than 413 K, material Bi0.4Sb1.6Te3 presented a higher efficiency compared to material Bi2Te3. The latter demonstrated that considering a material with constant properties overestimated the actual performance of TEGs. Overall, the material Bi2Te3 registered 35% more electric power generation and conversion efficiency compared to the material Bi0.4Sb1.6Te3.

On the other hand, the Fourier effect featured the most significant influence on the electrical generation capacity of TEGs (0-140 W/mm2), followed by the Peltier effect (0-0.16 W/mm2) and the Joule effect (0-0.02 W/mm2).

Between the examined materials with variable properties, it was proven that Bi0.4Sb1.6Te3 achieved a higher performance compared to material Cu11NiSb4S13. On average, the material Bi0.4Sb1.6Te3 increases the energy conversion efficiency up to 25% when compared to the material Cu11NiSb4S13. In conclusion, the study of material properties for TEG design using numerical simulations proved to be a cost-effective tool to evaluate the overall performance of this component in a reliable manner.

Acknowledgements

The authors would like to acknowledge the Universidad del Atlántico, Universidad Francisco de Paula Santander, and Sphere Energy company for their support in the development of this investigation.

References

[1] G.E. Valencia Ochoa, A.E. Benavides Gamero and J.M. Camargo Vanegas, "Vanegas, A world overview of organic Rankine cycle as waste heat recovery alternative", *Respuestas*, vol. 24, pp. 6–13, 2019. https://doi.org/10.22463/0122820x.1843.

[2] J.J. García Pabón, "Phase-out of high GWP refrigerants in refrigeration systems: Status of process in Colombia", *Respuestas*, 24, pp. 65–74, 2019. https://doi.org/10.22463/0122820x.1832.

[3] J. Duarte, G. Amador, J. Garcia, A. Fontalvo, R. Vasquez Padilla, M. Sanjuan and A. Gonzalez Quiroga, "Auto-ignition control in turbocharged internal combustion engines operating with gaseous fuels", Energy, 71, pp. 137–147, 2014. https://doi.org/10.1016/j.energy.2014.04.040.

[4] F.E. Moreno-García, J.J. Ramírez-Matheus and O.D. Ortiz-Ramírez, "Sistema de supervisión y control para un banco experimental de refrigeración por compresión", *Respuestas*, 21, pp. 97, 2016. https://doi.org/10.22463/0122820x.641.

[5] M.G. Francisco, B.F. Enio and B. V Jos, "Controladores fuzzy adaptativos para la optimización de un sistema chiller", *Respuestas*, 16, pp. 5–12, 2011. https://doi.org/10.22463/r.v16i1.406.

[6] E.D. Rincón Castrillo, J.R. Bermúdez Santaella, L.E. Vera Duarte and J.J. García Pabón, "Modeling and simulation of an electrolyser for the production of HHO in Matlab- Simulink®", *Respuestas*, 24, pp. 6–15, 2019. https://doi.org/10.22463/0122820x.1826.

[7] S. Şevik, "An analysis of the current and future use of natural gas-fired power plants in meeting electricity energy needs: The case of Turkey", Renewable & Sustainable Energy Reviews, 52, pp. 572–586, 2015. https://doi.org/10.1016/j.rser.2015.07.102.

[8] S. Mukherjee, A. Asthana, M. Howarth and R. Mcniell, "Waste heat recovery from industrial baking ovens", *Energy Procedia*, 123, pp. 321–328, 2017. https://doi.org/10.1016/j.egypro.2017.07.259.

[9] S. Ganguly, A. Date and A. Akbarzadeh, "Heat recovery from ground below the solar pond", *Solar Energy*, 155, pp. 1254–1260, 2017. https://doi.org/10.1016/j.solener.2017.07.068.

[10] B. Orr, A. Akbarzadeh, M. Mochizuki and R. Singh, "A review of car waste heat recovery systems utilising thermoelectric generators and heat pipes", *Applied Thermal Engineering*, 101, pp. 490–495, 2016. https://doi.org/10.1016/j.applthermaleng.2015.10.081.

[11] O. Högblom and R. Andersson, "A simulation framework for prediction of thermoelectric generator system performance", *Applied Energy*. 180, pp. 472–482, 2016. https://doi.org/10.1016/j.

apenergy.2016.08.019.

[12] Y. Zhang, X. Wang, M. Cleary, L. Schoensee, N. Kempf and J. Richardson, "High-performance nanostructured thermoelectric generators for micro combined heat and power systems", *Applied Thermal Engineering*, 96, pp. 8–87, 2016. https://doi.org/10.1016/j.applthermaleng.2015.11.064.

[13] S. Wu, H. Zhang and M. Ni, "Performance assessment of a hybrid system integrating a molten carbonate fuel cell and a thermoelectric generator", *Energy*, 112, pp. 520–527, 2016. https://doi.org/10.1016/j.energy.2016.06.128.

[14] Y. Wang, Y. Shi, D. Mei and Z. Chen, "Wearable thermoelectric generator to harvest body heat for powering a miniaturized accelerometer", *Applied Energy*, 215, pp. 690–698, 2018. https://doi.org/10.1016/j.apenergy.2018.02.062.

[15] A. Allouhi, A. Boharb, T. Ratlamwala, T. Kousksou, M.B. Amine, A. Jamil and A.A. Msaad, "Dynamic analysis of a thermoelectric heating system for space heating in a continuous-occupancy office room", *Applied Thermal Engineering*, 113, pp. 150–159, 2017. https://doi.org/10.1016/j.applthermaleng.2016.11.001.

[16] C. Lertsatitthanakorn, "Electrical performance analysis and economic evaluation of combined biomass cook stove thermoelectric (BITE) generator", *Bioresource Technology*, 98, pp. 1670–1674, 2007. https://doi.org/10.1016/j.biortech.2006.05.048.

[17] G. Komisarchik, Y. Gelbstein and D. Fuks, "Solubility of Ti in thermoelectric PbTe compound", *Intermetallics*, 89, pp. 16–21, 2017. https://doi.org/10.1016/j.intermet.2017.05.016.

[18] H. Choi, K. Jeong, J. Chae, H. Park, J. Baeck, T.H. Kim, J.Y. Song, J. Park, K.-H. Jeong and M.-H. Cho, "Enhancement in thermoelectric properties of Te-embedded Bi2Te3 by preferential phonon scattering in heterostructure interface", *Nano Energy*, 47, pp. 374–384, 2018. https://doi.org/10.1016/j.nanoen.2018.03.009.

[19] Q. Zhang, H. Wang, W. Liu, H. Wang, B. Yu, Q. Zhang, Z. Tian, G. Ni, S. Lee, K. Esfarjani and G. Chen, Z. Ren, "Enhancement of thermoelectric figure-of-merit by resonant states of aluminium doping in lead selenide", *Energy & Environmental Science Home*, 5, pp. 5246–5251, 2012. https://doi.org/10.1039/C1EE02465E.

[20] J.-C. Diez, S. Rasekh, M.A. Madre, M.A. Torres and A.E. Sotelo, "High thermoelectric performances of Bi–AE–Co–O compounds directionally growth from the melt", *Boletín de la Sociedad Española de Cerámica y Vidrio*, 57, pp. 1–8, 2018. https://doi.org/10.1016/j.bsecv.2017.10.003.

[21] Y. Lei, C. Cheng, Y. Li, R. Wan and M. Wang, "Microwave synthesis and enhancement of thermoelectric figure of merit in half-Heusler TiNiSb x Sn 1−x", *Ceramics International*, 43, pp. 9343–9347, 2017. https://doi.org/10.1016/j.ceramint.2017.04.100.

[22] Z. Li, Y. Chen, J.-F. Li, H. Chen, L. Wang, S. Zheng and G. Lu, "Systhesizing SnTe nanocrystals leading to thermoelectric performance enhancement via an ultra-fast microwave hydrothermal method", *Nano Energy*, 28, pp. 78–86, 2016. https://doi.org/10.1016/j.nanoen.2016.08.008.

[23] J.-F. Li, W.-S. Liu, L.-D. Zhao and M. Zhou, "High-performance nanostructured thermoelectric materials", *NPG Asia Materials*, 2, pp. 152–158, 2010. https://doi.org/10.1038/asiamat.2010.138.

[24] P. Fernández-Yañez, O. Armas, A. Capetillo and S. Martínez-Martínez, "Thermal analysis of a hermoelectric generator for light-duty diesel engines", *Applied Energy*, 226, pp. 690–702, 2018. https://doi.org/10.1016/j.apenergy.2018.05.114.

[25] N. Muralidhar, M. Himabindu and R.V. Ravikrishna, "Modeling of a hybrid electric heavy duty vehicle to assess energy recovery using a thermoelectric generator", *Energy*, 148, pp. 1046–1059, 2018. https://doi.org/10.1016/j.energy.2018.02.023.

[26] J.-H. Meng, X.-X. Zhang and X.-D. Wang, "Characteristics analysis and parametric study of a thermoelectric generator by considering variable material properties and heat losses", *International Journal of Heat and Mass Transfer*, 80, pp. 227–235, 2015. https://doi.org/10.1016/j.ijheatmasstransfer.2014.09.023.

[27] W.-H. Chen, S.-R. Huang, X.-D. Wang, P.-H. Wu and Y.-L. Lin, "Performance of a thermoelectric generator intensified by temperature oscillation", Energy, 133, pp. 257–269, 2017. https://doi.org/10.1016/j.energy.2017.05.091.

[28] W. Bai, X. Yuan and X. Liu, "Numerical investigation on the performances of automotive thermoelectric generator employing metal foam", *Applied Thermal Engineering*, 124, pp. 178–184, 2017. https://doi.org/10.1016/j.applthermaleng.2017.05.146.

[29] K. Tappura, "A numerical study on the design trade-offs of a thin-film thermoelectric generator for large-area applications", *Renewable Energy*, 120, pp. 78–87,2018. https://doi.org/10.1016/j.renene.2017.12.063.

[30] W.-H. Chen, C.-C. Wang, C.-I. Hung, C.-C. Yang and R.-C. Juang, "Modeling and simulation for the design of thermal-concentrated solar thermoelectric generator", *Energy*, 64, pp. 287–297, 2014. https://doi.org/10.1016/j.energy.2013.10.073.

[31] X.-D. Wang, Y.-X. Huang, C.-H. Cheng, D. Ta-Wei Lin and C.-H. Kang, "A three-dimensional numerical modeling of thermoelectric device with consideration of coupling of temperature field and electric potential field", *Energy*, 47, pp. 488–497, 2012. https://doi.org/10.1016/j.energy.2012.09.019.

[32] J.-H. Meng, X.-D. Wang and X.-X. Zhang, "Transient modeling and dynamic characteristics of thermoelectric cooler", *Applied Energy*, 108, pp. 340–348, 2013. https://doi.org/10.1016/j.apenergy.2013.03.051.

[33] S. Battiston, C. Fanciulli, S. Fiameni, A. Famengo, S. Fasolin and M. Fabrizio, "One step synthesis

and sintering of Ni and Zn substituted tetrahedrite as thermoelectric material", *Journal of Alloys and Compounds*, 702, pp. 75–83, 2017. https://doi.org/10.1016/j.jallcom.2017.01.187.

[34] Y.H. Yeo and T.S. Oh, "Thermoelectric properties of p-type (Bi,Sb)2Te3 nanocomposites dispersed with multiwall carbon nanotubes", *Materials Research Bulletin*, 58, pp. 54–58, 2014. https://doi.org/10.1016/j.materresbull.2014.04.046.

[35] W.-H. Chen, S.-R. Huang and Y.-L. Lin, "Performance analysis and optimum operation of a thermoelectric generator by Taguchi method", *Applied Energy*, 158, pp. 44–54, 2015. https://doi.org/10.1016/j.apenergy.2015.08.025.

[36] W.-H. Chen, C.-Y. Liao and C.-I. Hung, "A numerical study on the performance of miniature thermoelectric cooler affected by Thomson effect", *Applied Energy*, 89, pp. 464–473, 2012. https://doi.org/10.1016/j.apenergy.2011.08.022.

[37] W.-H. Chen, P.-H. Wu and Y.-L. Lin, "Performance optimization of thermoelectric generators designed by.multi-objective genetic algorithm", *Applied Energy*, 209, pp. 211–223, 2018. https://doi.org/10.1016/j.apenergy.2017.10.094.